Structure and Properties of the $[Ru(bpy)(CN)_4]^{2-}$ Complex and Its Solvent Environment: X-ray Diffraction and Density Functional Study

Tünde Megyes,[†] Gábor Schubert,[†] Margit Kovács,[‡] Tamás Radnai,*[,†] Tamás Grósz,[†] Imre Bakó,[†] Imre Pápai*[,†] and Attila Horváth*[,‡]

Chemical Research Center, Hungarian Academy of Sciences, Budapest, P.O. Box 17, H-1525 Hungary, and Department of General and Inorganic Chemistry, University of Veszprém, P.O. Box 158, Veszprém, H-8201 Hungary

Received: May 15, 2003; In Final Form: July 23, 2003

The structure of $[Ru(bpy)(CN)_4]^{2-}$ and its solvent shell in aqueous solution has been investigated by the X-ray diffraction technique. The characteristic bond lengths of the complex obtained by this method are in good agreement with those determined by a single-crystal X-ray study. The number of solvent molecules of the hydration shell has been determined. Three water molecules are arranged near to each cyanide ligand. The average distance between the nitrogen atoms of the cyanides and the oxygen atoms of these solvent molecules is found to be 3.2 Å. To examine this specific solvent−solute interaction, DFT calculations were performed on the gas phase complex and on its partially hydrated cluster models $[Ru(bpy)(CN)_4]^{2-}\cdot(H_2O)_n$ ($n = 4, 8$). These calculations confirmed the relatively strong CN···H−OH hydrogen bonds. It has also been demonstrated that the hydrogen bond is notably weaker in the triplet excited state than in the ground state of the complex. The lengthening of the N···H bonds due to the formation of the triplet excited complex is about 0.05 Å, and an appreciable influence on the second hydration shell is also demonstrated by the increase of the related O···H bond, which is at least 0.02 Å longer in the excited state.

1. Introduction

Synthesis of $K_2[Ru(bpy)(CN)_4]\cdot 2H_2O$ was reported in 1986.[1] The complex of C_{2v} symmetry having only one chromophoric ligand is considered as the simplest molecule within the class of ruthenium(II) polypyridine photosenzitizers of excellent spectroscopic, photophysical, photochemical, and electrochemical properties for conversion and storage of solar energy and as a unit of polynuclear and supramolecular species in which the centers of metal complexes or other types of molecules are bridged by cyanide ligands.[2,3]

The electronic spectra of the complex in the visible range are dominated by $t_{2g} \rightarrow \pi^*$ MLCT transitions with a maximum at 400 nm in water. The higher energy MLCT band appears as a shoulder (300 nm) of the intense intraligand $\pi \rightarrow \pi^*$ transition in the UV spectrum. The electronic structure of the ground state and the nature and the mutual arrangement of the relatively low energy excited states of ruthenium(II) polypyridine complexes are the focus of theoretical calculations aimed at providing an understanding of the properties of the MLCT excited state. The important role of mixing between t_{2g} (donor) and ligand π^* (acceptor) orbitals and the combination of the α- and β-type pyridine orbitals of the polypyridine ligands such as bipyridine have been widely demonstrated.[5] The semiempirical CINDO/S+Cl method was used to compare the electronic structure and the relative arrangement of the MLCT and d−d electronically excited states and the differences in energies of the singlet and triplet MLCT excited states of the series of $[Ru(bpy)(CN)_4]^{2-}$, $[Ru(bpy)_2(CN)_2]$, and $[Ru(bpy)_3]^{2+}$ complexes in which 2.028 and 1.16 Å bond lengths for Ru−C and C−N, respectively, were considered for the mixed ligand complexes.[6] These bond lengths are in a good agreement with that determined by an X-ray diffraction study of a $(PPN)_2[Ru(bpy)(CN)_4]\cdot 2CH_3CN\cdot 2(CH_3CH_2)_2O\cdot 2H_2O$ single crystal[7] (PPN^+: bis(triphenylphosphine) iminium).

MLCT absorption bands exhibit an extremely pronounced solvatochromic behavior.[1,4] The red-shift correlates with a decreasing acceptor number (AN) of the solvent. The emission band ($^3\pi^* \rightarrow t_{2g}$) peaking at 630 nm in aqueous solution is not so sensitive to the AN of the solvent. The effect of pH on absorption and emission spectra and on the lifetime of the excited $[Ru(bpy)(CN)_4]^{2-}$ has been demonstrated.[2b] It was also pointed out that the excited-state protonation of the complex in sulfuric acid aqueous solutions starts at significantly higher acidities than the ground-state protonation. These observations indicate the stronger basicity of the complex in the ground state than in the excited state. The specific solute−solvent interaction is usually considered to be predominated by H-bonds in protic solvents. The strong hydrogen bond interactions between the cyanide ligands of the complex and the ammonium groups of polyaza macrocycles ([24]ane-$[N_6H_6]^{6+}$ and [32]ane-$[N_8H_8]^{8+}$) provide the stability of supercomplexes.[3] The photophysics of these supercomplexes have been studied by various time-resolved techniques and compared with those of the $[Ru(bpy)(CN)_4]^{2-}$. Among these techniques, laser-induced optoacoustic spectroscopy proved to be very useful to demonstrate the role of the hydrogen bonded water molecule in the nonradiative deactivation of the ^{3}MLCT excited state of the ruthenium complex.

The temperature-dependent luminescence lifetime and quantum yield measurements and the external magnetic field

* Corresponding authors. E-mail addresses: attila@vegic.sol.vein.hu (A.H.), radnai@chemres.hu (T.R.), and papai@chemres.hu (I.P.). A.H. fax number: 36 88 427 915.

[†] Hungarian Academy of Sciences, Budapest.

[‡] University of Veszprém.

10.1021/jp0353439 CCC: $25.00
Published on Web 10/24/2003

TABLE 1: Physical Properties of the $K_2[Ru(bpy)(CN)_4]$ Solutions Studied: Salt Concentration c, Mass Density ρ, Linear X-ray Absorption Coefficient μ, and Atomic Number Density ρ_0

c (mol·dm^{-3})	ρ (g·cm^{-3})	μ (cm^{-1})	ρ_0 (cm^{-24})
0.428	1.139	2.542	0.1033
0.856	1.250	3.995	0.1036

modulated electron-transfer studies for $[Ru(bpy)(CN)_4]^{2-}$ dissolved in both water and D_2O indicated that the rate of photophysical processes and the rate of electron transfer from the triplet excited state to an electron acceptor molecule, such as methyl viologen (MV^{2+} = 1,1′-dimethyl-4,4′-dipyridinium), are strongly influenced by the H/D bond network in the solvent, and the solvent also has an impact on the H/D bond between the solvent molecules and the nitrogen atom of the CN ligand coordinated to the ruthenium center.[8]

In the present contribution, results of X-ray diffraction investigations on an aqueous solution of $[Ru(bpy)(CN)_4]^{2-}$ are discussed and compared with the crystal structure of the complex. The aim of this study was to obtain reliable data for the arrangement of the water molecule in the first shell of the solvents. To get further information on the specific solvent−solute interaction governed by the hydrogen bond, density functional theory (DFT) calculations were performed for the ground state and for the lowest energy triplet excited-state complex, and the variations of the CN···H−OH hydrogen bonds of the singlet ground-state complex due to formation of the lowest energy triplet exited state were also calculated for $[Ru(bpy)(CN)_4]^{2-}\cdot(H_2O)_n$ (n = 4, 8) clusters.

2. Experimental and Data Treatment

2.1. Synthesis. $K_2[Ru(bpy)(CN)_4]\cdot 2H_2O$ (bpy = 2,2′-bipyridine) was synthesized by a method published by Jiwan et al.[9] The purity of the complex was checked by elemental analysis and UV−vis absorption and emission, IR, Raman, and H NMR spectroscopies.[1,3a,4d,10] The results of these experiments match those reported in the literature.

2.2. X-ray Measurements and Data Treatment. The X-ray scattering measurements were carried out on solutions of the ruthenium complex in water of two different concentrations (Table 1).

The measurements were performed with a Θ−Θ goniometer by using the symmetrical transmission geometry and Mo Kα radiation (with λ = 0.7107 Å wavelength) with a graphite monochromator in the diffracted beam at ambient temperature (24 ± 1 °C). The liquid sample holder had plane-parallel windows prepared from 6.3 μm thick Mylar foils. The scattering angle range of measurement covered $1.28° \le 2\Theta \le 120°$, corresponding to the range $0.2\ \text{Å}^{-1} \le k \le 15.3\ \text{Å}^{-1}$ of the scattering variable $k = (4\pi/\lambda)\sin\Theta$. More than 100 000 counts were collected, in several repeated runs (20 000 counts at each point and each run), at 150 discrete angles selected in $\Delta k \approx 0.1\ \text{Å}^{-1}$ steps. The technical details and data treatment were essentially the same as those described previously.[11]

The measured intensities were corrected for background, polarization, absorption, and Compton scattering.[12] The Compton contribution was evaluated by a semiempirical method in order to account for the monochromator discrimination.[13] The Compton intensities needed for the corrections were calculated with analytical formulas.[14,15] The experimental structure function was derived by

$$h(k) = \frac{I(k) - \sum_\alpha x_\alpha f_\alpha^{\,2}(k)}{M(k)} \quad (1)$$

where $I(k)$ is the corrected coherent intensity of the scattered beam normalized to electron units;[16] $f_\alpha(k)$ and x_α are the scattering amplitude and mole fraction for a type of α particle, respectively; and $M(k)$ is the modification function $M(k) = \{1/[\sum x_\alpha f_\alpha(k)]^2\}\exp(-0.01k^2)$. The coherent scattering amplitudes of the ions and the water molecules were computed according to an analytical formula suggested by Hajdu[14] and Cromer et al.[17] The parameters were taken from the *International Tables for X-ray Crystallography*.[18] The water molecules were treated as sets of independent atomic scattering units.

The experimental pair correlation function was computed from the structure function $h(k)$ by Fourier transformation according to

$$g(r) = 1 + \frac{1}{2\pi^2 r\rho_0}\int_{k_{min}}^{k_{max}} kh(k)\,M(k)\sin(kr)\,\mathrm{d}k \quad (2)$$

where r is the interatomic distance, k_{min} and k_{max} are the lower and upper limits of the experimental data, and ρ_0 is the bulk number density of the stoichiometric units. After repeated Fourier transformations when the nonphysical peaks appearing in the $g(r)$ at small r values were removed, the structure function was corrected for residual systematic errors.[19] Contributions to the experimental $h(k)$ function due to the intramolecular interactions in the bipyridine molecules centered at about 1.40 and 2.45 Å in the $g(r)$ function were calculated by using the single-crystal X-ray diffraction data in ref 7 and were subtracted.

The radial distribution function is often presented in an alternative form of $D(r) - 4\pi r^2\rho_0$, and it is calculated from $g(r)$ functions as $D(r) = 4\pi r^2\rho_0 g(r)$.

The experimental structure function has been compared to a theoretical one, the latter being based on a suitably chosen geometrical model. The model has been evaluated by a least-squares refinement procedure with minimizing the sum of squared residuals,

$$S_{res} = \sum_{k_{min}}^{k_{max}} k^2[h(k)_{exp} - h(k)_{calc}]^2 \quad (3)$$

The theoretical intensities $h(k)$ were calculated by the formulas

$$h(k) = h_d(k) + h_c(k) \quad (4)$$

$$h_d(k) = \sum_{\alpha\beta} x_\alpha n_{\alpha\beta} f_\alpha f_\beta M(k)\frac{\sin(kr_{\alpha\beta})}{kr_{\alpha\beta}}\exp\left(-\frac{\sigma_{\alpha\beta}^2}{2}k^2\right) \quad (5)$$

$$h_c = \sum_{\alpha\beta} 4\pi\rho_0 x_\alpha x_\beta f_\alpha f_\beta M(k) \times \frac{kR_{\alpha\beta}\cos(kR_{\alpha\beta}) - \sin(kR_{\alpha\beta})}{k^3}\exp\left(\frac{\Gamma_{\alpha\beta}^{\,2}}{2}k^2\right) \quad (6)$$

where α and β refer to scattering centers of different chemical types. The first term $h_d(k)$ is related to the short-range interactions characterized by the interatomic distance $r_{\alpha\beta}$, its root-mean-square deviation $\sigma_{\alpha\beta}$, and the coordination number $n_{\alpha\beta}$. The second term $h_c(k)$ arises from the interaction between particles of uniform distribution beyond a certain discrete distance. $R_{\alpha\beta}$

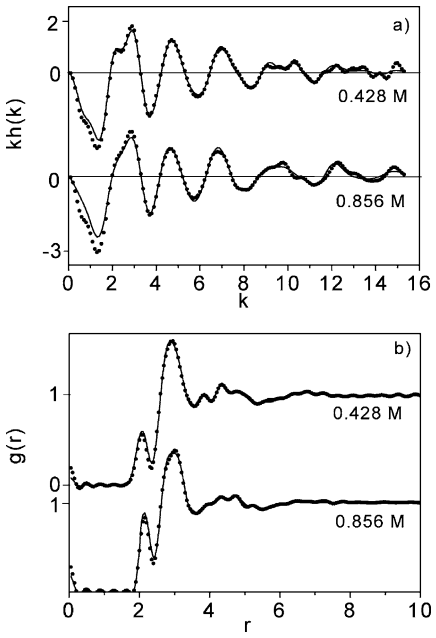

Figure 1. Structure functions $h(k)$ multiplied by k (a) and pair correlation functions $g(r)$ (b) for ruthenium bipyridine complex solutions in water. The experimental values are given by dots, and the theoretical values are given by solid lines.

and $\Gamma_{\alpha\beta}$ define the boundary of the uniform distribution of α- and β-type distances and its root-mean-square deviation.

2.3. Computational Details of the DFT Study. The electronic structures of the investigated complexes are described in terms of the Kohn−Sham formalism of DFT.[20] The energy gap between the luminescent excited state and the ground state for a given complex is estimated from the total electronic energies of the lowest lying triplet and singlet states calculated at the geometry-optimized structures.

Assuming a C_{2v} symmetry for the [Ru(bpy)(CN)$_4$]$^{2-}$ complex, full geometry optimization was first carried out for the singlet state at the B3LYP/SDD+ level of DFT, where B3LYP denotes the applied exchange-correlation hybrid functional[21,22] and SDD+ corresponds to the Stuttgart−Dresden relativistic small core ECP basis set for Ru[23] and the Dunning/Dunning-Hay DZ + polarization + diffuse all electron basis set for the remaining atoms.[24,25] The optimized geometry of the ground state ($^1A_1$) was used as an initial structure for optimization of the triplet states, of which the $^3B_2$ state turned out to be the lowest state.

To model the specific solute−solvent interaction, four water molecules were first attached to the $^1A_1$ and $^3B_2$ structures of Ru(bpy)(CN)$_4^{2-}$ via CN···H−OH type hydrogen bonds so as to maintain the C_{2v} symmetry of the Ru(bpy)(CN)$_4^{2-}$·(H$_2$O)$_4$ cluster. The influence of the second water molecule was also considered by constructing the Ru(bpy)(CN)$_4^{2-}$·(H$_2$O)$_8$ cluster, where additional water molecules are bound to the O lone pairs of each CN-coordinated H$_2$O. The $^1A_1$ and $^3B_2$ states of the two models were geometry optimized at the B3LYP/SDD+ level of theory.

All calculations were performed with the Gaussian 98 software package.[26]

3. Results and Discussion

3.1. X-ray Diffraction Study of Aqueous Solutions of K$_2$[Ru(bpy)(CN)$_4$]. The experimental and theoretical X-ray structure functions, derived for solutions of both concentrations, are shown in Figure 1a. The first double peak—as is well-known from the experience with scattering patterns of hydrogen bonded liquids—is obviously predominated by the interference of scattering contributions of the bulk solutions. The same peak is observable in the structure functions of pure solvents as well (not shown here). The double peak feature is decreased by the increase of concentration.

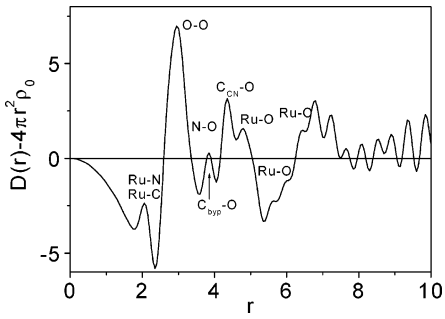

Figure 2. Difference radial distribution functions in the form of $D(r) - 4\pi r^2\rho_0$ for a 0.428 M ruthenium bipyridine complex solution in water. The expected main contributions of pair interactions are indicated by legends.

The $g(r)$ functions are shown in Figure 1b. For the first peak centered around 2 Å, intramolecular Ru−C and Ru−N interactions are responsible. An assignment based on a previous single-crystal X-ray study of the [Ru(bpy)(CN)$_4$]$^{2-}$ yields average Ru−C and Ru−N distances of 2.04 and 2.1 Å, respectively.

By the increase of concentration, the peak height increases, due to the increased weight of Ru−N and Ru−C type contributions to the scattering pattern. A rather complex main peak can be observed in the range 2.5−3.5 Å. This peak can be assigned to a great number of interactions, namely, C−C and Ru···C intramolecular distances in the ruthenium bipyridine complex, the O···O interaction in the bulk, the K···O interaction, and the N···O interaction from the N···H−O hydrogen bond from the first hydration shell around the complex. Another broad peak appears in the range 4−6 Å. These peaks are difficult to resolve because of their complexity, and therefore, a model analysis can only tentatively reveal the major contributions to them. A better visualized but still qualitative analysis can be given with the construction of the difference radial distribution function $D(r) - 4\pi r^2\rho_0$, where the experimental function for pure water (not shown in this paper) is subtracted from the one for the solution, accounting for the difference in number densities. Figure 2 shows the difference radial distribution function. Some of the most important proposed assignments to contributions are denoted in the figure. A peak around 2.05 Å is observable, which can be assigned to Ru−C and Ru−N interactions.

The intermolecular N···O interaction is partly responsible for the peak appearing at 3.20 Å. The peak at 3.7 Å and the other one at 4.15 Å are probably predominated by C$_{bpy}$···O interactions and C$_{CN}$···O interactions, arising from the first hydration shell of the complex. Around 4.8, 6, and 6.4 Å, further peaks can be observed, for which mostly Ru···O interactions are responsible.

The structural parameters obtained from the least-squares fit of the structure functions $h(k)$ shown in Figure 1a for the aqueous solution of K$_2$[Ru(bpy)(CN)$_4$] are given in Table 2. An initial geometrical picture was assumed for the structure at the beginning of the fitting procedure. An octahedral arrangement of the four cyanide ligands and the bipyridine was supposed around the ruthenium. An examination of the weights of the contributions to the structure function shows that the ion−ion type interactions are negligible compared to the others. Accordingly, in $h_d(k)$ and $h_c(k)$ functions (eqs 5 and 6), one contribution for each type of interaction, listed in Table 2, was involved.

TABLE 2: Structural Parameters for the 0.428 and 0.856 M Aqueous Solutions of the Ruthenium Bipyridine Complex with the Estimated Errors in the Last Digits[a]

type of bonds and atomic distances	*r* (Å) 0.428 M	*r* (Å) 0.856 M	*N*	σ (Å)
Ru—C	2.04 (0.01)	2.05 (0.01)	4	0.20
Ru—N	2.10 (0.03)	2.13 (0.05)	2	0.15
Ru—N*	3.18	3.19	4	0.20
C—C*	2.89	2.90	2.5	0.20
C≡N*	2.93	2.97	2	0.20
Ru···C_{2byp}*	2.98	2.91	2	0.20
Ru···C_{3byp}*	4.25	4.19	2	0.25
Ru···C_{4byp}*	4.89	4.84	2	0.30
Ru···C_{5byp}*	4.36	4.33	2	0.25
Ru···C_{6byp}*	3.09	3.05	2	0.20
C···C_{2byp}*	3.62	3.59	2	0.25
C···C_{3byp}*	4.70	4.69	2	0.30
C···C_{4byp}*	5.31	5.29	2	0.40
C···C_{5byp}*	4.81	4.80	2	0.30
C···C_{6byp}*	3.72	3.69	2	0.25
Solvent and K				
O···O	2.83 (0.01)	2.80 (0.01)	3.29 (0.08)	0.20
K···O	2.90 (0.01)	2.90 (0.01)	6	0.20
Hydrate Sphere				
N···O	3.21 (0.05)	3.20 (0.05)	3.0 (0.5)	0.20
C···O	4.15 (0.05)	4.18 (0.05)	3.0 (0.5)	0.25
Ru···O	6.25 (0.05)	6.25 (0.05)	12 (1)	0.40
Water Molecules Positioned to the Faces of the Octahedron				
C···O	3.79 (0.08)	3.78 (0.06)	6	0.30
Ru—O	4.81 (0.05)	4.80 (0.05)	6	0.35
Hydrate Sphere around the Bipyridine				
C—O	3.70 (0.03)	3.70 (0.03)	2.1 (0.5)	0.3
Ru···O*	5.9	6.0	8	0.4
Ru···O*	6.45	6.45	8	0.4
Ru···O*	6.8	6.8	4	0.4

[a] For the two solutions only the distances differ; the coordination numbers (*n*) and the mean square deviations are the same. The contributions marked with an asterisk were treated as dependent parameters.

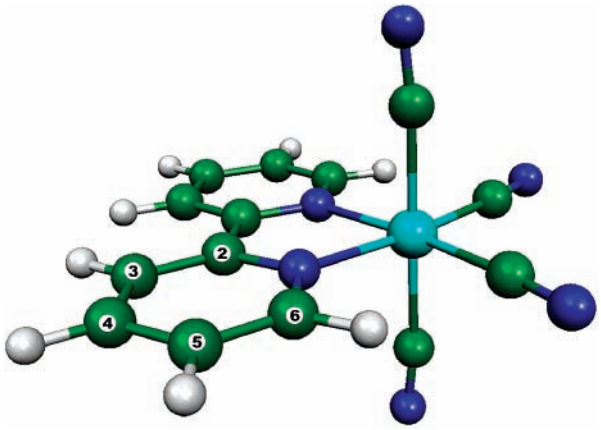

Figure 3. Ball and stick representation of the $[Ru(bpy)(CN)_4]^{2-}$ complex.

The fitting procedure resulted in 2.04 ± 0.01 Å and 2.10 ± 0.03 Å for the Ru—C and the Ru—N distances, respectively. These data are in good agreement with the data of the single-crystal X-ray diffraction study[7] and correspond to the octahedral arrangement of these six atoms around the ruthenium, as shown in Figure 3.

The doubling of the concentration of the complex leads to a very small increase in the distance estimated between the central atom and the donor atom of the coordinated ligands (Table 2). In addition, some shortening in distance between the C atoms of the bpy and the metal center is also indicated. On the other hand, this increase in concentration will change neither the number nor the orientation of molecules around $[Ru(bpy)(CN)_4]^{2-}$. The complex is surrounded by water molecules, forming thus a second shell around the central ruthenium atom. About three water molecules are located at a distance of 3.20 Å from the nitrogen atom of each cyanide group. These water molecules are positioned at 4.15 and 6.25 Å from the C_{CN} and Ru, respectively. Six water molecules are located at the faces of the octahedron, at a distance of 3.79 Å from the C_{CN} and 4.81 Å from the Ru atoms. About 21 water molecules can be found in the neighborhood of the bipyridine ligand at a distance of 3.7 Å from the carbon atoms. Taking into account the geometry of the bipyridine ring and the C_{byp}···O distance, the Ru···O distances will fall in the range around 5.9, 6.45, and 6.8 Å. The O···O interaction appears around 2.83 Å while the O···O coordination number sums up to 3.29 for a solution of 0.428 solute concentration. For comparison it is worth noting that in pure liquid water the corresponding O···O distance is 2.85 Å and the coordination number is about 4.1.[27] The shortening of the O···O distance and the lowering of the coordination number can be explained by the reduction of the original bulk structure, which is also confirmed by data obtained for a 0.856 M solution. The K^+ ion, hydrated by with six water molecules, was found at a distance of 2.9 Å from the ion. It is very difficult to derive more information about the geometry of the hydration sphere of the K^+ ion due to the low weight of the potassium—water interaction to the overall scattering pattern.

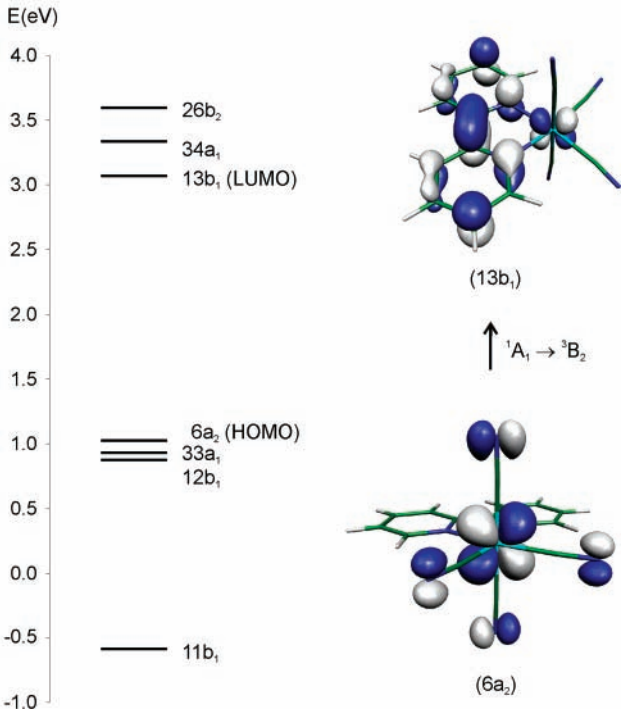

Figure 4. Kohn—Sham orbital energy diagram and the surface plot of frontier orbitals of the $[Ru(bpy)(CN)_4]^{2-}$ ($^1A_1$) complex.

3.2. Density Functional Study. (*a*) *$[Ru(bpy)(CN)_4]^{2-}$ Complex.* The electronic structure of the closed-shell $^1A_1$ ground state of the gas-phase complex is characterized by the presence of three close-lying occupied molecular orbitals in the HOMO region ($12b_1$, $33a_1$ and $6a_2$; see Figure 4). These orbitals are, however, well separated both from the next doubly occupied orbital ($11b_1$) and from the lowest lying virtual orbital ($13b_1$). The three highest occupied orbitals have similar characters in that they are mixtures of Ru 4d and CN related N 2p orbitals, whereas the $13b_1$ orbital has predominantly a bpy character with a slight Ru 4d contribution. Our calculations show that the

TABLE 3: Selected Equilibrium Bond Lengths (in Å) for the $^1A_1$ and $^3B_2$ States of $[Ru(bpy)(CN)_4]^{2-}$

	$^1A_1$	[exp]	$^3B_2$
$Ru-C_{CN(eq)}$	2.02	[2.00]	2.02
$Ru-C_{CN(ax)}$	2.08	[2.07]	2.09
$Ru-N_{bpy}$	2.10	[2.11]	2.15
$C-C_{bpy}$	1.47	[1.49]	1.43
$C-N_{ax}$	1.18	1.15	1.18
$C-N_{eq}$	1.18	1.14	1.18

TABLE 4: Net Charges (Q) and the Population of the 5s and 4d Ru Orbitals As Obtained from Natural Population Analysis Carried out for the $^1A_1$ and $^3B_2$ States of $[Ru(bpy)(CN)_4]^{2-}$

	$^1A_1$	$^3B_2$
	Ru Atom	
Q(Ru)	−0.09	+0.29
el configuration	$5s^{0.42}4d^{7.58}$	$5s^{0.43}4d^{7.21}$
	CN Ligands	
$Q(C_{ax})$	+0.12	+0.10
$Q(C_{eq})$	+0.20	+0.18
$Q(N_{ax})$	−0.64	−0.57
$Q(N_{eq})$	−0.65	−0.59
	bpy Ligand	
Q(bpy)	+0.02	−0.50

lowest lying triplet state of $[Ru(bpy)(CN)_4]^{2-}$ is $^3B_2$. This state can be derived from the ground state by the $(6a_2)^2(13b_1)^0 \rightarrow (6a_2)^1(13b_1)^1$ excitation, which corresponds to a metal-to-ligand charge-transfer process as judged from the nature of the involved orbitals ($t_{2g}^6 \rightarrow t_{2g}^5\pi^{*1}$). The energy splitting between the $^1A_1$ and $^3B_2$ states is predicted to be 6300 cm^{-1}, which is rather far from the energy difference estimated by the Franck−Condon analysis of the phosphorescence spectra ($t_{2g}^5\pi^{*1} \rightarrow t_{2g}^6$) of the complex in aqueous solution. However, we do not expect the present level of theory to provide accurate predictions for the energy gap; moreover, we show below that solute−solvent interactions alter significantly the calculated energy splitting.

Some selected equilibrium structural parameters of the two states are collected in Table 3. The optimized structures indicate that the $Ru-C_{CN}$ bond distances are not altered upon the $^1A_1 \rightarrow {}^3B_2$ excitation; however, owing to the Ru−bpy antibonding nature of the $13b_1$ orbital, the $Ru-N_{bpy}$ bond weakens in the triplet state. Note also that the shortening of the C−C bond linking the two pyridine units in bpy is also consistent with the MO picture, since $13b_1$ describes a π bonding between these atoms.

To quantify the electronic rearrangements in the $^1A_1 \rightarrow {}^3B_2$ excitation process, natural population analysis[28] was carried out for the equilibrium structures (see Table 4). As expected, a notable increase of the electron density on the bpy ligand is observed on the excitation, which is accompanied by the reduction of the Ru 4d population and also by the decrease of the negative charge on the cyanides' N atoms. As demonstrated below, these variations in the electron density distribution have an important impact on the bonding interactions operating between the CN groups and the water molecules in the solution phase.

(b) $[Ru(bpy)(CN)_4]^{2-}\cdot(H_2O)_n$ Clusters. The optimized structures of the $[Ru(bpy)(CN)_4]^{2-}\cdot(H_2O)_4$ and $[Ru(bpy)(CN)_4]^{2-}\cdot(H_2O)_8$ clusters are depicted in Figure 5. These cluster models are, of course, too small to represent the full hydration network around the $[Ru(bpy)(CN)_4]^{2-}$ ion, which is rather complicated, as has been demonstrated by the X-ray diffraction study of aqueous solutions. However, they may serve to reveal structural and energetic changes occurring in the $^1A_1 \rightarrow {}^3B_2$ excitation process.

In accordance with the reduced basicity of the cyanide N atoms in the excited state of the gas-phase $[Ru(bpy)(CN)_4]^{2-}$ complex, the CN···H−OH hydrogen bonds are found to be notably weaker in the $^3B_2$ states of the hydrated models. For instance, the N···H bonds in the triplet states of the $[Ru(bpy)(CN)_4]^{2-}\cdot(H_2O)_4$ and $[Ru(bpy)(CN)_4]^{2-}\cdot(H_2O)_8$ clusters are lengthened by about 0.05 Å relative to those in the ground-state structures. Moreover, this effect seems to have an appreciable influence on the next hydration shell as well, since the related O···H hydrogen bonds in $[Ru(bpy)(CN)_4]^{2-}\cdot(H_2O)_8$ are at least 0.02 Å longer in the excited state. Considering the change in the bond lengths of the complex and in hydrogen bonds according to the $[Ru(bpy)(CN)_4]^{2-}\cdot(H_2O)_8$ cluster, a structural volume change of ∼15 cm^3 mol^{-1} can be estimated due to the formation of the triplet excited state. This structural volume change was measured by laser-induced optoacoustic spectroscopy (LIOAS) and was explained on the basis of hydrogen bond interactions between the complex and the first solvation shell.[3b,30] The results obtained by our cluster model suggest that the influence of the excitation is extended over the second layer of the water molecules connected by hydrogen bonds to cyanide ligands of the ruthenium complex. The calculated interaction energies[29] support these trends in that the average H_2O binding energy in $[Ru(bpy)(CN)_4]^{2-}\cdot(H_2O)_4$ is about 2 kcal mol^{-1} (∼700 cm^{-1}) lower in the $^3B_2$ state, and the

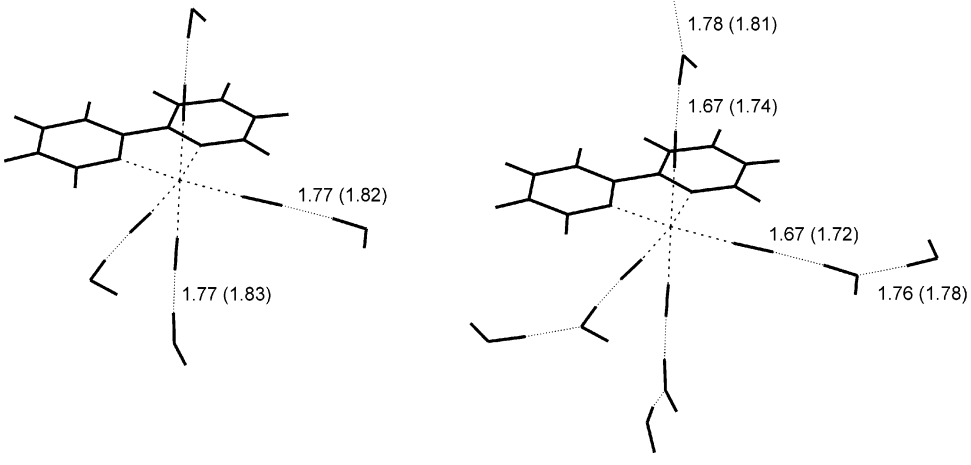

Figure 5. Optimized C_{2v} structures of the $[Ru(bpy)(CN)_4]^{2-}\cdot(H_2O)_4$ and $[Ru(bpy)(CN)_4]^{2-}\cdot(H_2O)_8$ clusters with selected bond lengths.

H_2O-H_2O interactions in $[Ru(bpy)(CN)_4]^{2-}\cdot(H_2O)_8$ are reduced by about 1 kcal mol^{-1} ($\sim$350 cm^{-1}) in the excited state.

We thus find that the ground state of the $[Ru(bpy)(CN)_4]^{2-}$ complex is clearly more stabilized by the electrostatic interactions with the protic solvent molecules than its excited state, which implies that the $^1A_1 - {}^3B_2$ energy splittings calculated for the hydrated models are considerably larger than the gas-phase value. Our present calculations give 9200 cm^{-1} and 10570 cm^{-1} for the $^1A_1 \rightarrow {}^3B_2$ excitation energies for the $[Ru(bpy)(CN)_4]^{2-}\cdot(H_2O)_4$ and $[Ru(bpy)(CN)_4]^{2-}\cdot(H_2O)_8$ clusters, respectively. Hence, one can estimate a 3500 cm^{-1} increase of the energy gap between the $^3B_2$ and $^1A_1$ states due to $[Ru(bpy)(CN)_4]^{2-}\cdot(H_2O)_8$ cluster formation by hydrogen bonds. A rather similar shift ($\sim$3000 cm^{-1}) in the maximum of the emission spectrum was observed for a vapochromically active film of anhydrous $(PPN)_2[Ru(bpy)(CN)_4]$ when it was exposed to 100% relative humidity.[7] The FT-IR spectral studies of the anhydrous $(PPN)_2[Ru(bpy)(CN)_4]$ and its partially hydrated forms revealed that the initial waters of hydration were associated with hydrogen bonding to the cyanide ligands trans to bpy, which was followed by the hydrogen bonding of water molecules to the axial cyanide ligands, and the changes were smaller and gradual with increasing humidity between 66 and 100%, which was associated with filling the cavity of $(PPN)_2[Ru(bpy)(CN)_4]$ with water molecules. These findings strongly suggest that our $[Ru(bpy)(CN)_4]^{2-}\cdot(H_2O)_8$ cluster is a reasonable model for analyzing the influence of the water molecules associated with cyanide ligands by hydrogen bonds. It is reasonable to suppose that such an interaction can play a crucial role not only in the energetics of the complex but also in the rate of nonradiative deactivation processes of the triplet excited state as well.

4. Conclusions

The structure of the $[Ru(bpy)(CN)_4]^{2-}$ complex and its solvent environment in water have been studied by X-ray diffraction. The structural parameters of the complex such as distances between the ruthenium center and the donor atoms of the coordinated ligands and the other characteristic distances within the complex anion determined by a fitting procedure are in good agreement with those of the single-crystal studies. It has been demonstrated that some of the water molecules form the hydration shell around the complex are oriented to given positions presumably by a specific solute−solvent interaction. So, three water molecules are localized near to the nitrogen atom of each cyanide ligand. In addition, six further water molecules are positioned on the six faces of the octahedron and quite a large number of solvent molecules are found around the bipyridine ligand. A relatively strong interaction between the protic solvent molecule and the nitrogen atom of the coordinated cyanide ligands of the ground-state complex has been proved by quantum chemical calculations using $[Ru(bpy)(CN)_4]^{2-}(H_2O)_4$ and $[Ru(bpy)(CN)_4]^{2-}(H_2O)_8$ clusters as model systems. The results obtained by the latter cluster predict an appreciable influence on the second hydration shell. The calculated stabilization of the complex in the ground state due to the hydrogen bond interactions between the first and second water molecules is about half of the value calculated for hydrogen bonding of the first solvent molecules to the complex. In addition, the structural changes occurring in the formation of the triplet exited MLCT state are pointed out on the O···H hydrogen bonds of the second water molecules attached to the first water molecules hydrogen bonded to the nitrogen atom of the coordinated cyanide ligands. These bonds are at least 0.02 Å longer in the excited state than in the ground state, while the increase in the N···H bonds is 0.05 Å.

Acknowledgment. Financial support by the Hungarian National Science Foundation (OTKA Nos. T35107 and M 27542) is gratefully acknowledged. The authors are very grateful to G. Lendvay for helpful discussions.

Supporting Information Available: Tables of Cartesian coordinates for the B3LYP/SDD+ optimized structures of the $[Ru(bpy)CN_2]^{2-}$ and $[Ru(bpy)(CN)_4]^{2-}\cdot nH_2O$ ($n = 4$ or 8) complexes. This material is available free of charge via the Internet at http://pubs.acs.org.

References and Notes

(1) Bignozzi, C. A.; Chiorboli, C.; Indelli, M. T.; Rampi Scandola, M. A.; Varani, G.; Scandola, F. *J. Am. Chem. Soc.* **1986**, *108*, 7872−7873.

(2) (a) Scandola, F.; Indelli, M. T. *Pure Appl. Chem.* **1988**, *60*, 973−980. (b) Indelli, M. T.; Bignozzi, C. A.; Marconi, A. M.; Scandola, F. In *Photochemistry and Photophysics of Coordination Compounds*; Yersin, H., Vogler, A., Eds.; Springer: Berlin, 1987; p 159.

(3) (a) Rampi, M. A.; Indelli, M. T.; Scandola, F.; Pina, F.; Parola, A. J. *Inorg. Chem.* **1996**, *35*, 3355−3361. (b) Borsarelli, C. D.; Braslavsky, S. E.; Indelli, M. T.; Scandola, F. *Chem. Phys. Lett.* **2000**, *317*, 53−58.

(4) (a) Indelli, M. T.; Bignozzi, C. A.; Marconi, A.; Scandola, F. *J. Am. Chem. Soc.* **1988**, *110*, 7381−7386. (b) Kato, M.; Yamauchi, S.; Hirota, N *J. Phys. Chem.* **1989**, *93*, 3422−3425. (c) Ülveczky, A.; Horváth, A. *Inorg. Chim. Acta* **1995**, *236*, 173−176. (d) Timpson, C. J.; Bignozzi, C. A.; Sullivan, B. P.; Kober, E. M.; Meyer, T. J. *J. Phys. Chem.* **1996**, *100*, 2915−2925.

(5) Endicott, J. F.; Schlegel, H. B.; Uddin, Md. J.; Seniveratne, D. S. *Coord. Chem. Rev.* **2002**, *229*, 95−106.

(6) Sizova, O. V.; Ivanova, N. V.; Nikolskii, A. B.; Panin, A. I.; Baranovskii, V. I.; Ershov, A. Yu. *Russ. J. Gen. Chem.* **1999**, *69*, 576−580.

(7) Evju, J. K.; Mann, K. R. *Chem. Mater.* **1999**, *11*, 1425−1433.

(8) (a) Kovács, M.; Horváth, A. *Inorg. Chim. Acta* **2002**, *335*, 69−76. (b) Fodor, L.; Ülveczki, A.; Horváth, A.; Steiner, U. E. *Inorg. Chim. Acta* **2002**, *338*, 133−141.

(9) Jiwan, J. H.; Wegewijs, B.; Indelli, M. T.; Scandola, F.; Braslavsky, S. E. *Recl. Trav. Chim. Pays-Bas* **1995**, *114*, 542−548.

(10) Maruyama, M.; Matsuzawa, H.; Kaizu, Y. *Inorg. Chim. Acta* **1995**, *237*, 159−162.

(11) Radnai, T.; Ohtaki, H. *Mol. Phys.* **1996**, *87*, 103−121.

(12) Hajdu, F.; Pálinkás, G. *J. Appl. Crystallogr.* **1972**, *5*, 395−401.

(13) Levy, H. A.; Danford, M. D.; Narten, A. H. *Oak Ridge Natl. Lab. Rep.* **1966**, Nr. 3960.

(14) Hajdu, F. *Acta Crystallogr.* **1972**, *A28*, 250−252.

(15) Pálinkás, G.; Radnai, T. *Acta Crystallogr.* **1976**, *A32*, 666−668.

(16) Krogh-Moe, K. J. *Acta Crystallogr.* **1956**, *2*, 951−953.

(17) Cromer, D. T.; Waber, J. T. *Acta Crystallogr.* **1965**, *18*, 104−109.

(18) *International Tables for X-ray Crystallography*; The Kynoch Press: 1974; Vol 4.

(19) Narten, A. H. *J. Chem. Phys.* **1979**, *70*, 299−304.

(20) Parr, R. G.; Yang, W. *Density-Functional Theory of Atoms and Molecules*; Oxford University Press: 1989.

(21) Becke, A. D. *J. Chem. Phys.* **1993**, *98*, 5648−5652.

(22) Lee, C.; Yang, W.; Parr, R. G. *Phys. Rev. B* **1988**, *37*, 785−789.

(23) Dolg, M.; Stoll, H.; Preuss, H.; Pitzer, R. M. *J. Phys. Chem.* **1993**, *97*, 5852−5859.

(24) Dunning, T. H., Jr. *J. Chem. Phys.* **1970**, *53*, 2823−2833.

(25) Dunning, T. H., Jr.; Hay, P. J. In *Methods of Electronic Structure Theory*; Schaefer, H. F., III, Ed.; Plenum Press: 1977; Vol. 3.

(26) Frisch, M. J.; Trucks, G. W.; Schlegel, H. B.; Scuseria, G. E.; Robb, M. A.; Cheeseman, J. R.; Zakrzewski, V. G.; Montgomery, J. A., Jr.; Stratmann, R. E.; Burant, J. C.; Dapprich, S.; Millam, J. M.; Daniels, A. D.; Kudin, K. N.; Strain, M. C.; Farkas, O.; Tomasi, J.; Barone, V.; Cossi, M.; Cammi, R.; Mennucci, B.; Pomelli, C.; Adamo, C.; Clifford, S.; Ochterski, J.; Petersson, G. A.; Ayala, P. Y.; Cui, Q.; Morokuma, K.; Rega, N.; Salvador, P.; Dannenberg, J. J.; Malick, D. K.; Rabuck, A. D.; Raghavachari, K.; Foresman, J. B.; Cioslowski, J.; Ortiz, J. V.; Baboul, A. G.; Stefanov, B. B.; Liu, G.; Liashenko, A.; Piskorz, P.; Komaromi, I.; Gomperts, R.; Martin, R. L.; Fox, D. J.; Keith, T.; Al-Laham, M. A.; Peng, C. Y.; Nanayakkara, A.; Challacombe, M.; Gill, P. M. W.; Johnson, B.; Chen, W.; Wong, M. W.; Andres, J. L.; Gonzalez, C.; Head-Gordon, M.; Replogle, E. S.; Pople, J. A. *Gaussian 98*, Revision A.11.4; Gaussian Inc.: Pittsburgh, PA, 2002.

(27) (a) Narten, A. H.; Levy, H. A. *J. Chem. Phys.* **1971**, *55*, 2263. (b) Ludwig, R. *Angew. Chem., Int. Ed.* **2001**, *39*, 1808−1827.

(28) Reed, A. E.; Curtiss, L. A.; Weinhold, F. *Chem. Rev.* **1988**, *88*, 899−926.

(29) The average H_2O binding energies (calculated from the corresponding electronic total energies as $-(1/4)\{E_{tot}[Ru(bpy)(CN)_4^{2-}\cdot(H_2O)_4] - E_{tot}[Ru(bpy)(CN)_4^{2-}] - 4E_{tot}[H_2O]\}$) in the $^1A_1$ and $^3B_2$ states of $Ru(bpy)(CN)_4^{2-}\cdot(H_2O)_4$ are -6120 and -5390 cm^{-1}, whereas the average binding energy of the second-shell H_2O molecules (defined as $-(1/4)\{E_{tot}[Ru(bpy)(CN)_4^{2-}\cdot(H_2O)_8] - E_{tot}[Ru(bpy)(CN)_4^{2-}\cdot(H_2O)_4] - 4E_{tot}[H_2O]\}$) are -4510 and -4160 cm^{-1} for the $^1A_1$ and $^3B_2$ states, respectively.

(30) (a) Borsarelli, C. D.; Braslavsky, S. E. *J. Photochem. Photobiol., B: Biology* **1998**, *43*, 222−228. (b) Borsarelli, C. D.; Braslavsky, S. E. *J. Phys. Chem. B* **1998**, *102*, 6231−6238.